

Dissipative dynamics of Bose condensates in optical cavities

Peter Horak and Helmut Ritsch

Institut für Theoretische Physik, Universität Innsbruck, Technikerstrasse 25, A-6020 Innsbruck, Austria

(Received 16 February 2000; published 8 January 2001)

We study the zero-temperature dynamics of Bose-Einstein condensates in driven high-quality optical cavities in the limit of large atom-field detuning in a one-dimensional model. We calculate the stationary ground state and the spectrum of coupled atom and field mode excitations for standing-wave cavities as well as for traveling-wave cavities. Finite cavity response times lead to damping or controlled amplification of these excitations. Analytic solutions in the Lamb-Dicke expansion are in good agreement with numerical results for the full problem and show that oscillation frequencies and the corresponding damping rates are qualitatively different for the two cases.

DOI: 10.1103/PhysRevA.63.023603

PACS number(s): 03.75.Fi, 05.30.Jp, 32.80.Pj, 42.50.Vk

I. INTRODUCTION

The experimental realization of Bose-Einstein condensation (BEC) in dilute atomic gases a couple of years ago [1] as a consequence of improved cooling and trapping techniques has dramatically boosted the study of ultracold atoms. Today, BEC is a widespread tool and a huge range of new phenomena has been investigated experimentally and theoretically, see e.g., Refs. [2–4] for recent overviews. In this context the interaction of BEC's with laser light and optical lattices has been studied intensively [5–10] and effects such as the reduction of the speed of light by many orders of magnitude [11] and the occurrence of super-radiance [12] have been found. Recently the optical creation of vortices [13,14] has been demonstrated and many more intriguing effects have been theoretically predicted.

In parallel, the field of cavity quantum electrodynamics, which studies the interaction of matter with one or a few single light modes, has reached such a level of sophistication that the interaction of light with the internal and external degrees of freedom of a single neutral particle can be observed and controlled in a very precise way [15]. For optical fields, trapping and cooling of a single atom in a cavity mode has been demonstrated [16,17]. It is thus a logical next step to combine these two successful techniques and study the interaction of a BEC with a high finesse optical cavity, that is, the strong coupling of a far detuned optical mode to the dynamics of a condensate described by its macroscopically occupied wave function [18]. Several groups have already been working along these lines and, for example, predicted the amplification of matter waves [19] and the occurrence of dressed condensates [20]. In the extreme limit one could envisage a large atomic cloud trapped and manipulated with a single photon.

In this paper we extend our recently proposed scheme for cooling one or a few atoms in high-quality optical cavities [21,22] to the case of a BEC. This requires a quantum-mechanical treatment of the external degrees of freedom and the inclusion of atom-atom interactions. The system under investigation is a Bose-Einstein condensate interacting with the mode (the two modes) of a driven standing-wave cavity (ring cavity). The properties of such a system as a measuring

device for condensates have been discussed previously [18,23].

We will investigate the ground-state and collective excitations [24–27] of the coupled condensate-light field system in the optical potential of the cavity. Because of the strong coupling of the condensate wave function to the cavity modes, an oscillation of the condensate also leads to an oscillation of the intracavity light fields. Accordingly, the oscillation frequencies of the collective excitations are shifted with respect to an external optical potential of fixed depth, i.e., the optical potential formed by a free space standing wave. Furthermore, for appropriately chosen parameters the dissipative dynamics of the cavity due to cavity decay gives rise to damping of the condensate excitations without incoherent spontaneous emission. We analyze this damping mechanism and study its parameter dependence by numerical solutions of the coupled equations of motion as well as by analytic solutions of a simplified model based on the Lamb-Dicke expansion.

This paper is organized as follows. In Sec. II we discuss the case of a condensate interacting with the single mode of a standing-wave cavity. After presenting the set of coupled nonlinear equations of motion for the condensate and the light field, we discuss the numerical and analytical solutions for the ground state and the collective excitations. Section III investigates the more complicated situation of a condensate coupled to the two independent modes of an optical ring cavity. In Sec. IV we discuss the influence of binary collisions between the atoms within the condensate on the excitation frequencies and damping rates. Finally, we summarize our results in Sec. V.

II. BEC IN STANDING-WAVE CAVITY

Let us first consider the case of a Bose-Einstein condensate interacting with a single standing-wave mode. The cavity mode is assumed for all times to be in a coherent state $|\alpha(t)\rangle$ and the condensate is described by a single wave function $|\psi(t)\rangle$ for all N particles, which is a good approximation at zero temperature. This means that we factorize the quantum state of the system and thus neglect any entanglement between the condensate and the cavity field which might build up in the course of the time evolution. This

simplification is only justified in the limit of a large photon number $|\alpha|^2$. To avoid spontaneous emission, we assume a very large detuning of the light field from the atomic resonance. More precisely, we assume that the cavity decay is the dominant incoherent process in the system and we thus require that $\kappa \gg N\Gamma s$, where κ is the cavity decay rate, N the number of atoms in the condensate, Γ the spontaneous decay rate of the atoms, and s the atomic saturation parameter. After adiabatic elimination of the atomic excited states we obtain the following equations of motion,

$$\frac{d}{dt}\alpha(t) = [i\Delta_c - iN\langle U(\hat{x}) \rangle - \kappa]\alpha(t) + \eta, \quad (1a)$$

$$i\frac{d}{dt}\psi(x,t) = \left\{ \frac{\hat{p}^2}{2m} + |\alpha(t)|^2 U(x) + N g_{coll} |\psi(x,t)|^2 \right\} \psi(x,t). \quad (1b)$$

Here Δ_c is the detuning of the pump field from the cavity mode, $U(x) = U_0 \cos^2(kx)$ is the optical potential formed by a single cavity photon ($U_0 = \hbar g_0^2 / \Delta_a$ with the single-photon Rabi frequency g_0 and the atom-pump detuning Δ_a), and η describes the action of the driving laser. The expectation value $\langle U(\hat{x}) \rangle$ has to be taken with respect to the momentary wave function $|\psi(t)\rangle$. Equation (1b) is the well known Gross-Pitaevskii equation (GPE) for a condensate in an external field, which in our case depends on the momentary field intensity $|\alpha(t)|^2$. The last term in the GPE models the interaction of atoms within the condensate, where g_{coll} is related to the s -wave scattering length a by $g_{coll} = 4\pi\hbar^2 a / (mw^2)$, where w denotes the transverse size of the condensate.

Note that we are using a simplified one-dimensional version of the GPE here. For this approximation to hold we require that the transverse extension w of the condensate is smaller than the waist of the cavity field and approximately constant during the observation time of the system. This could be achieved, at least in principle, by a transverse confining potential such as a magnetic field or a condensate trapped in the center of a donut mode laser beam. Alternatively, in the case of red detuning of the pumping laser with respect to the atomic resonance, one could envisage three-dimensional (3D) trapping of the condensate at the antinodes of the cavity field itself. For blue detuning one could think of a condensate that is freely expanding in the transverse directions while falling through the cavity. Then the one-dimensional model only holds for a restricted period of time until the above condition on the transverse confinement is no longer fulfilled. However, in these cases without additional transverse trapping mechanism, the electric-field gradient of the cavity mode is about two orders of magnitude larger along the cavity axis than in the transverse directions, and thus the dipole forces on the condensate in the longitudinal direction are much stronger too. For instance, for the cavity parameters of the single-atom experiments by Rempe and co-workers [16] we find a ratio of 150 between the longitudinal and the transverse trapping frequencies. Hence the effects discussed in this paper and any transverse effects occur

on completely different time scales and could thus be easily separated. We hence chose a simplified one-dimensional model, which does not correspond to a specific experimental setup but demonstrates the main physical effects of the condensate-cavity interaction more clearly.

Equations (1) are two coupled nonlinear equations describing the dynamics of the compound system formed by the condensate and the cavity field [23]. The most interesting effects occur for parameters where the coupling between these equations significantly changes the system behavior. We thus impose the condition $NU_0 \gg \kappa$, which guarantees that the presence of the condensate shifts the cavity frequency efficiently into or out of resonance with the driving field. At the same time the optical potential depth $|\alpha|^2 U_0$ should be large enough to provide at least a few bound states for the atoms. Limitations and the interesting parameter regimes for this model have been discussed in Ref. [23].

A. Ground state

In order to obtain the ground state of the compound condensate-cavity system, we have to find the stationary solution of the system of coupled nonlinear equations (1). This can be done by elimination of $|\alpha(t)|^2$ in Eq. (1b) using Eq. (1a), and a subsequent numerical solution of the resulting nonlinear equation for the ground-state wave function with the method of steepest descent. This consists of a numerical propagation of the GPE in imaginary time $\tau = it$ until the wave function converges to a stationary state.

In this paper we will concentrate on the case of $U_0 > 0$ where the potential minima coincide with the nodes of the field (low-field seeking atoms). The ground-state wave function will thus be localized at the field nodes, thereby minimizing the coupling of the condensate to the light field. For a cavity resonant with the driving field, this means that the photon number is maximum for the stationary ground state. Any excitation of the condensate will then lead to a smaller cavity field.

As expected we find that the ground-state wave function becomes better localized for stronger driving fields η and larger optical potentials U_0 . On the other hand, a strong atom-atom repulsion (large positive values of g_{coll}) increases the width of the BEC wave function and thus counteracts the confining effect of the potential. This, in due course, leads to an increased coupling of the BEC to the cavity field and hence a smaller field intensity. A more detailed analysis of the ground-state wave function $\psi_0(x)$, its energy μ , and the stationary field intensity $|\alpha_0|^2$ has been given in Ref. [23].

B. Collective excitations

Let us now turn to weak excitations of the condensate from the ground state. First, we will calculate the spectrum of collective excitations of the condensate. In contrast to fixed external fields, the trapping potential in the cavity depends on the BEC wave function. Hence, excitations include small deviations of the wave function *and* the cavity field α from their respective stationary state. We may thus write $\psi(x,t) = \exp(-i\mu t)[\psi_0(x) + \delta\psi(x,t)]$ and $\alpha(t) = \alpha_0 + \delta\alpha(t)$.

For convenience we have already included the ground-state time evolution into the ansatz for the wave function here. Inserting this into Eqs. (1) and linearizing in $\delta\psi$ and $\delta\alpha$ we obtain

$$i\frac{d}{dt}\delta\alpha = [-\Delta_c + N\langle\psi_0|U(\hat{x})|\psi_0\rangle - i\kappa]\delta\alpha + N\alpha_0\langle\delta\psi|U(\hat{x})|\psi_0\rangle + N\alpha_0\langle\psi_0|U(\hat{x})|\delta\psi\rangle, \quad (2a)$$

$$i\frac{d}{dt}\delta\psi = \left\{ \frac{\hat{p}^2}{2m} + |\alpha_0|^2 U + 2Ng_{coll}|\psi_0|^2 - \mu \right\} \delta\psi + Ng_{coll}\psi_0^2\delta\psi^* + \alpha_0 U\psi_0\delta\alpha^* + \alpha_0^* U\psi_0\delta\alpha. \quad (2b)$$

For large κ (more precisely, for $1/\kappa$ much smaller than the time scale of the condensate motion), the cavity field follows adiabatically the changes of the wave function and thus $\delta\alpha$ can be adiabatically eliminated. In this case one recovers the limit of Ref. [23].

In general the linearized time evolution couples the deviations $\delta\psi$ and $\delta\alpha$ also to their complex conjugates. In order to obtain excitation eigenstates, i.e., periodic solutions, we thus have to use the simultaneous ansatz

$$\begin{aligned} \delta\psi &= e^{-\gamma}[e^{-i\nu t}\delta\psi_+(x) + e^{i\nu t}\delta\psi_-(x)^*], \\ \delta\alpha &= e^{-\gamma}[e^{-i\nu t}\delta\alpha_+ + e^{i\nu t}\delta\alpha_-^*]. \end{aligned} \quad (3)$$

The collective excitations are thus defined as the solutions of the eigenvalue problem

$$\omega \begin{pmatrix} \delta\alpha_+ \\ \delta\alpha_- \\ \delta\psi_+(x) \\ \delta\psi_-(x) \end{pmatrix} = \mathbf{M} \begin{pmatrix} \delta\alpha_+ \\ \delta\alpha_- \\ \delta\psi_+(x) \\ \delta\psi_-(x) \end{pmatrix}, \quad (4)$$

where \mathbf{M} is easily obtained from Eqs. (2) as a non-Hermitian matrix. The complex eigenvalues have the form $\omega_n = \nu_n - i\gamma_n$, where ν_n is the oscillation frequency of the n th collective excitation and γ_n the corresponding damping rate. Note that, depending on the parameters, negative damping rates are possible, leading to an exponential growth of the collective excitations. In this case the assumption of small deviations from the ground state imposed above only holds for very short times. Hence by changing some cavity parameters we can switch between stable and unstable cases and generate controlled excitations of the condensate and study their decay. In the following we will, however, concentrate on the case of positive γ_n and therefore damped excitations.

Physically this damping arises from a kind of Sisyphus mechanism. For cavity damping rates κ of the order of the oscillation frequencies ν_n , the cavity field follows with a certain delay the changes of the condensate wave function. By properly choosing the system parameters, having the wave function climb up the potential hills at higher cavity

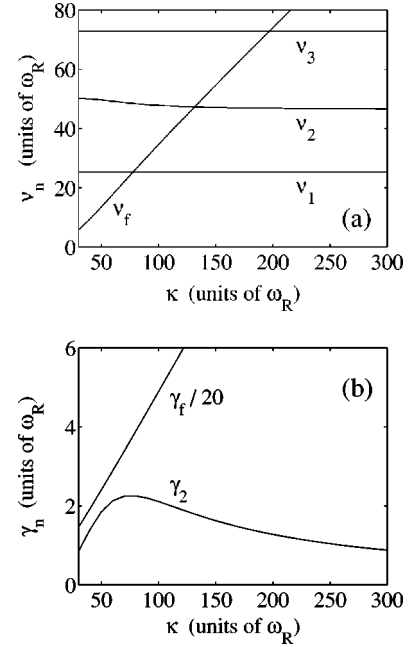


FIG. 1. Collective condensate excitations: (a) frequencies ν_n and (b) decay rates γ_n vs cavity decay rate κ . The parameters are $g_{coll} = \Delta_c = 0$, $NU_0 = 10\kappa$, and $\eta^2 = 20\kappa N\omega_R$, where $\omega_R = \hbar k^2/(2m)$.

field intensities and run down at lower intensities can be achieved on average. The condensate thus loses potential energy, which is carried away by the cavity output field without an intrinsic decoherence of the condensate.

Furthermore it should be emphasized that the appearance of a damping rate in the linearized equations (2) is a purely quantum feature related to the width of the atomic wave function. In the semiclassical limit of a pointlike particle, the self-consistent ground state yields a particle exactly located at a node of the cavity and hence all expectation values in Eq. (2a) vanish. Thus the cavity field decouples from the atomic degrees of freedom and no damping of the atomic motion occurs to lowest order in the elongation x . This is in contrast to the case of a ring cavity as will be shown in the following section.

In Fig. 1 we show the oscillation frequencies and damping rates of the lowest collective excitations obtained numerically by calculating the eigenvalues of Eq. (4) on a spatial grid. The eigenvalues are plotted as a function of the cavity decay rate κ . Note that in order to keep the optical potential constant, we also have to scale the driving field η^2 and the optical potential per photon U_0 proportional to κ . For clarity, atomic collisions are neglected here and their effects will be discussed separately in Sec. IV.

We see that there exists one single eigenvalue $\omega_f = \nu_f - i\gamma_f$ that scales approximately proportional to κ in contrast to all of the other eigenvalues. This specific excitation of the system corresponds to an eigenmode where mainly the cavity field oscillates and the condensate wave function is only weakly perturbed. In fact, Eq. (2a) shows that in the case where the atoms are well localized at the nodes of the field

(semiclassical limit), the cavity mode decouples from the matter wave function and the eigenvalue is given by $\omega_f = -\Delta_c - i\kappa$.

Second, we notice that out of the other modes ν_n , $n = 1, 2, \dots$, the ones with odd indices are independent of κ and their damping rates vanish. This effect is due to the spatial symmetry of the problem considered here. For all parameters we find that the ground-state wave function ψ_0 is symmetric in the position x . Thus for all *antisymmetric* excitations the expectation values in Eq. (2a) vanish and the light field decouples. Therefore these odd ($n = 1, 3, \dots$) excitations are the same as for a trap of constant light intensity and hence there is no Sisyphus damping mechanism at work. Consequently only the lowest *symmetric* collective excitations are significantly altered by the interaction with the damped cavity mode. We will discuss the parameter dependence of the excitation $n=2$ by using an approximate analytic solution in the next section.

Let us finally emphasize that the oscillation frequency and the damping rate of the symmetric collective excitations can be monitored nondestructively via the cavity output intensity.

C. Harmonic-oscillator approximation

In order to gain more insight into the parameter dependence of this damping mechanism, we will now analytically solve an approximate model of our system. To this end we expand the optical potential $U(x) = U_0 \cos^2(kx)$ with $U_0 > 0$ up to second order around the nodes of the field, i.e., we set $U(x) = U_0(kx)^2$ and assume $g_{coll} = 0$, i.e., no atom-atom interaction. For simplicity we will also assume $\Delta_c = 0$.

The ground state of the Schrödinger equation (1b) is thus the well-known harmonic oscillator ground state that depends on the cavity field $|\alpha|^2$ in a parametric way. After inserting this wave function in the expectation value in Eq. (1a) we obtain an equation for the self-consistent cavity field with the solution

$$|\alpha_0|^2 = \frac{\eta^2}{\kappa^2} - \frac{N^2 U_0 \omega_R}{4 \kappa^2}, \quad (5)$$

where $\omega_R = \hbar k^2 / (2m)$ is the recoil frequency. The corresponding harmonic-oscillator frequency is then

$$\omega_0 = 2 \omega_R \sqrt{|\alpha_0|^2 U_0 / \omega_R} \quad (6)$$

and the ground-state energy is $\mu = \omega_0 / 2$.

For the collective excitations we now have to solve Eqs. (2) with the harmonic potential. The last expectation value of Eq. (2a) thus reads

$$\begin{aligned} \langle \psi_0 | U(\hat{x}) | \delta\psi \rangle &= U_0 \langle \psi_0 | (k\hat{x})^2 | \delta\psi \rangle \\ &= -U_0 \frac{\omega_R}{\omega_0} \langle \psi_0 | (a - a^\dagger)^2 | \delta\psi \rangle, \end{aligned} \quad (7)$$

where we have used the standard relation between the position operator \hat{x} and the ladder operators a and a^\dagger of the

harmonic oscillator. From this we see that the cavity field only couples to wave-function deviations $\delta\psi$ containing the ground-state ψ_0 and/or the second excited state ψ_2 of the harmonic oscillator. Most of the harmonic-oscillator excited states are thus unperturbed and we find the collective excitations of the form $\delta\psi_+(x) = \psi_n$, $\delta\alpha_+ = \delta\alpha_- = \delta\psi_-(x) = 0$ with the positive eigenvalues $\omega = n\omega_0$ for $n=1$ and $n \geq 3$. Analogously there exist excitations with negative eigenvalues $\omega = -n\omega_0$ of the form $\delta\psi_-(x) = \psi_n$, $\delta\alpha_+ = \delta\alpha_- = \delta\psi_+(x) = 0$. Hence, in addition to the antisymmetric states already found to decouple previously, also the higher lying symmetric states decouple in the harmonic approximation. Therefore these symmetric excitations are only damped due to the anharmonicity of the potential and due to atomic collisions in the full model.

The remaining (and most interesting) collective excitations are finally found by restricting the wave functions $\delta\psi_\pm$ in Eq. (4) to the two-dimensional Hilbert space spanned by ψ_0 and ψ_2 . The resulting 6×6 matrix has two zero eigenvalues and the other four eigenvalues have to be found by solving the fourth-order polynomial equation

$$\begin{aligned} &(-i\kappa + NU_0(\omega_R/\omega_0) - \omega)(-i\kappa - NU_0(\omega_R/\omega_0) - \omega) \\ &\times (\omega^2 - 4\omega_0^2) - 4(NU_0\omega_R)^2 = 0. \end{aligned} \quad (8)$$

This gives us the (complex) eigenvalues ω_f and ω_2 and their counterparts of negative frequency. Although an analytic solution of Eq. (8) is possible in principle, the resulting expressions are rather long and do not provide much insight. Instead, we calculate the eigenvalue ω_2 in the limit of large κ as in Fig. 1, i.e., by keeping U_0/κ and η^2/κ constant. The zeroth order in this expansion in ω/κ yields the leading order of the frequency

$$\nu_2 = 2\omega_0 \sqrt{1 - \frac{N^2 U_0 \omega_R}{4\eta^2}} \quad (9)$$

and the first order gives the leading order of the decay rate

$$\gamma_2 = \frac{4N^2 U_0^2 \omega_R^2}{\kappa^3} \left(1 - \frac{N^2 U_0 \omega_R}{4\eta^2} \right)^2. \quad (10)$$

Equation (9) gives a quantitative explanation for the frequency shift of ν_2 according to the coupling of the BEC and the cavity mode as compared to the value $2\omega_0$ for the case of a harmonic-oscillator potential of fixed photon number. We also see that the small variation of ν_2 in Fig. 1(a) for small values of κ are in fact of the order $1/\kappa^2$. Equation (10) leads to the asymptotic behavior like $1/\kappa$ for the decay rate γ_2 in Fig. 1(b). In the limit of a strong driving field the frequency ν_2 of the second collective excitation approaches the harmonic-oscillator value. Simultaneously the damping rate γ_2 tends towards a constant nonvanishing value, which is proportional to the square of the atom number N . A higher condensate density thus significantly increases the damping of the collective excitation.

III. BEC IN A RING CAVITY

In this section we will now discuss the case of a BEC in a ring cavity. In this case the condensate is coupled to the two independent travelling wave modes α_{\pm} . For simplicity we will assume in the following that both modes of the cavity are driven with the same pumping rate η [28]. Therefore the equations of motion read

$$\frac{d}{dt}\alpha_{\pm}(t)=[i\Delta_c-iNU_0-\kappa]\alpha_{\pm}(t)-iNU_0\langle e^{\mp 2ik\hat{x}}\rangle\alpha_{\mp}+\eta, \quad (11a)$$

$$i\frac{d}{dt}\psi(x,t)=\left\{\frac{\hat{p}^2}{2m}+U_0|\alpha_+(t)e^{ikx}+\alpha_-(t)e^{-ikx}|^2+Ng_{coll}|\psi(x,t)|^2\right\}\psi(x,t). \quad (11b)$$

Hence, in general, the condensate will scatter light between the left and right running waves and induce a strong coupling. This gives additional degrees of freedom to the system compared to the standing-wave case. For example, in addition to intensity shifts the condensate can also induce a relative phase shift between the two modes, which changes the position of the potential wells. Analogously, the minima can also be controlled externally by the relative phase of the two driving fields, which allows to selectively excite antisymmetric excitations.

Considering the important role that the spatial symmetry plays for the standing-wave cavity, we will now change the description of the cavity modes by $\alpha_s=\alpha_++\alpha_-$ and $\alpha_a=\alpha_+-\alpha_-$, which have symmetric and antisymmetric mode functions, respectively. In this new basis Eqs. (11) read

$$\frac{d}{dt}\alpha_s(t)=[i\Delta_c-iNU_0-iNU_0\langle\cos(2k\hat{x})\rangle-\kappa]\alpha_s(t)+NU_0\langle\sin(2k\hat{x})\rangle\alpha_a(t)+2\eta, \quad (12a)$$

$$\frac{d}{dt}\alpha_a(t)=[i\Delta_c-iNU_0+iNU_0\langle\cos(2k\hat{x})\rangle-\kappa]\alpha_a(t)-NU_0\langle\sin(2k\hat{x})\rangle\alpha_s(t), \quad (12b)$$

$$i\frac{d}{dt}\psi(x,t)=\left\{\frac{\hat{p}^2}{2m}+U_0|\alpha_s(t)\cos(kx)+i\alpha_a(t)\sin(kx)|^2+Ng_{coll}|\psi(x,t)|^2\right\}\psi(x,t). \quad (12c)$$

Note that because of the assumption of a single pumping rate η for α_+ and α_- , in the new basis only the symmetric mode α_s is pumped. The antisymmetric mode α_a only contains photons that have been scattered by the condensate out of α_s .

A. Ground state

For the calculation of the ground state of the compound system formed by the BEC and the cavity modes we will again assume the case $U_0>0$. We then find that the ground-state wave function is localized at the nodes of the driven mode α_s and is symmetric in x . Thus the expectation values of $\sin(2kx)$ in Eqs. (12) vanish and Eq. (12b) decouples. The stationary state of the antisymmetric mode is therefore given by $\alpha_{a,0}=0$. Equations (12a) and (12c) then reduce to the Eqs. (1) for the standing-wave cavity if one identifies the parameters

$$\begin{aligned} 2U_0^r &= U_0^s, \\ |\alpha_s^r|^2/2 &= |\alpha^s|^2, \\ \sqrt{2}\eta^r &= \eta^s, \end{aligned} \quad (13)$$

for the ring cavity and the standing-wave cavity, respectively. The ground state of the system can thus be obtained by using our previous results for the standing-wave cavity and all of the discussions there equally apply to the ground state in the ring cavity.

B. Collective excitations

The collective excitations are calculated with the same method as in the preceding section by linearization of the equations of motion (12) in small deviations of $|\psi\rangle$, α_s , and α_a from their stationary states $|\psi_0\rangle$, $\alpha_{s,0}$, and 0. Choosing the ground-state wave function to be real and taking its symmetry into account we obtain

$$i\frac{d}{dt}\delta\alpha_s=[-\Delta_c+2NU_0\langle\psi_0|\cos^2(k\hat{x})|\psi_0\rangle-i\kappa]\delta\alpha_s+2NU_0\alpha_{s,0}[\langle\delta\psi|\cos^2(k\hat{x})|\psi_0\rangle+c.c.], \quad (14a)$$

$$i\frac{d}{dt}\delta\alpha_a=[-\Delta_c+2NU_0\langle\psi_0|\sin^2(k\hat{x})|\psi_0\rangle-i\kappa]\delta\alpha_a-NU_0\alpha_{s,0}[\langle\delta\psi|\sin(2k\hat{x})|\psi_0\rangle+c.c.], \quad (14b)$$

$$i\frac{d}{dt}\delta\psi=\left\{\frac{\hat{p}^2}{2m}+|\alpha_{s,0}|^2U_0\cos^2(k\hat{x})+2Ng_{coll}|\psi_0|^2-\mu\right\}\delta\psi+Ng_{coll}\psi_0^2\delta\psi^*+U_0\cos^2(k\hat{x})\psi_0(\alpha_{s,0}\delta\alpha_s^*+c.c.)-\frac{i}{2}U_0\sin(2k\hat{x})\psi_0(\alpha_{s,0}\delta\alpha_a^*-c.c.). \quad (14c)$$

From these equations we see that the behavior of the excitation eigenstates strongly depends on their spatial symmetry.

For *symmetric* excitations $\delta\psi(x)$ the last expectation value in Eq. (14b) vanishes and the antisymmetric cavity mode decouples from the wave function. Hence in this case we find $\delta\alpha_a=0$. The equations of motion for $\delta\psi$ and $\delta\alpha_s$ then reduce to their standing-wave counterpart discussed in the previous section if one rescales the parameters as in Eq.

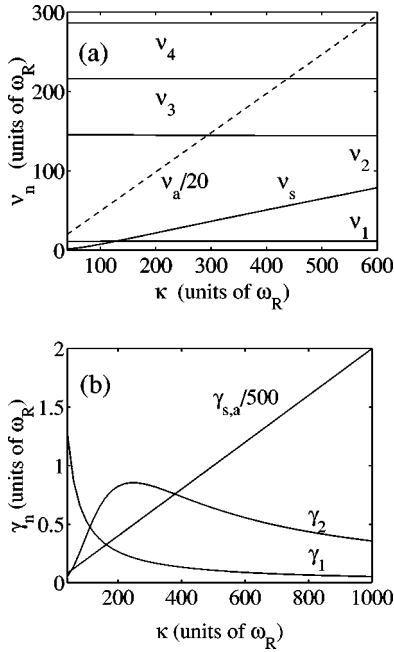


FIG. 2. Collective condensate excitations in a ring cavity: (a) frequencies ν_n and (b) decay rates γ_n vs cavity decay rate κ . The parameters are $g_{coll} = \Delta_c = 0$, $N U_0 = 5\kappa$, and $\eta^2 = 70\kappa N \omega_R$.

(13). The symmetric collective excitations are thus the same as those in a standing-wave cavity.

Analogously, for *antisymmetric* excitations $\delta\psi(x)$ the symmetric cavity mode decouples and therefore $\delta\alpha_s = 0$. We then find a new set of coupled equations for $\delta\psi$ and $\delta\alpha_a$. Thus, in contrast to the case of a standing-wave cavity, also the antisymmetric excitations are damped in a ring cavity. However, the damping mechanism is of completely different physical origin. Instead of the Sisyphus mechanism discussed above, here the coherent scattering of photons from the α_s cavity mode into the α_a mode is responsible for the damping. This leads to less severe requirements for the cavity parameters as we will see in the following subsection.

Figure 2 shows the spectrum of collective excitations of a Bose condensate in a ring cavity that is obtained from the numerical solution of Eqs. (14). First, we note that in contrast to the case of the standing-wave cavity we now find *two* modes with eigenvalues that scale proportional to the cavity decay rate κ . In the semiclassical limit (atoms well localized), these correspond to pure oscillations of the symmetric and antisymmetric field mode, respectively, and are thus labeled $\omega_s = \nu_s - i\gamma_s$ and $\omega_a = \nu_a - i\gamma_a$. The semiclassical limits of these eigenfrequencies are obtained from Eqs. (14) as $\omega_s = -\Delta_c - i\kappa$ and $\omega_a = -\Delta_c + 2NU_0 - i\kappa$. Although the damping rates of these modes are equal, we see that the different spatially dependent coupling to the atoms leads to a large difference in the oscillation frequencies.

For the parameters chosen in Fig. 2 the other oscillation frequencies ν_n , $n \geq 1$, are mainly independent of κ . However, whereas all frequencies with $n \geq 2$ are equally spaced and hence very well described by harmonic-oscillator states, the lowest frequency ν_1 is significantly shifted downwards. For the damping rates we find that only the two lowest ex-

citations exhibit relevant damping. However, the dependence of these damping rates on the system parameters is qualitatively different according to the different damping mechanisms. We will return to the discussion of these features in the following subsection where we derive analytic approximations for the eigenvalues. Notice finally that due to the relatively small damping rates for some parameter regimes these effects might be difficult to observe in a full three-dimensional (3D) experiment depending on the actual transverse dynamics.

C. Harmonic-oscillator approximation

Let us now calculate analytic estimates for the lowest oscillation frequencies and damping rates along the lines of Sec. II C. We will thus again assume $\Delta_c = g_{coll} = 0$.

As we have already seen, the calculation of the ground state and of the symmetric collective excitations can be reduced to the problem of the standing wave if the appropriate identification of the system parameters (13) is made. We can therefore use our previous results to obtain the self-consistent cavity field

$$|\alpha_{s,0}|^2 = \frac{4\eta^2}{\kappa^2} - \frac{N^2 U_0 \omega_R}{\kappa^2} \quad (15)$$

and the corresponding harmonic-oscillator frequency

$$\omega_0 = 2\omega_R \sqrt{|\alpha_{s,0}|^2 U_0 / \omega_R}. \quad (16)$$

For the lowest symmetric excitation, the expansion for large values of κ yields

$$\nu_2 = 2\omega_0 \sqrt{1 - \frac{N^2 U_0 \omega_R}{4\eta^2}} \quad (17)$$

and

$$\gamma_2 = \frac{16N^2 U_0^2 \omega_R^2}{\kappa^3} \left(1 - \frac{N^2 U_0 \omega_R}{4\eta^2} \right)^2. \quad (18)$$

Analogously, we can calculate the lowest antisymmetric excitation by expanding the expectation values in Eqs. (14b) and (14c) to lowest order in $k\hat{x}$. To this order only $\delta\psi$ and $\delta\psi^*$ proportional to the first harmonic-oscillator wave function ψ_1 couple to the cavity field $\delta\alpha_a$ and $\delta\alpha_a^*$ and we thus have to find the eigenvalues of a 4×4 matrix, that is, we must solve the characteristic polynomial

$$\begin{aligned} & [-i\kappa + 2NU_0(1 - \omega_R/\omega_0) - \omega] \\ & \times [-i\kappa - 2NU_0(1 - \omega_R/\omega_0) - \omega](\omega^2 - \omega_0^2) \\ & - 4(NU_0\omega_0)^2(1 - \omega_R/\omega_0) = 0. \end{aligned} \quad (19)$$

In the limit of $\kappa \rightarrow \infty$ (with constant U_0/κ and η^2/κ) this yields the oscillation frequency

$$\nu_1 = \omega_0 \sqrt{1 - \frac{4N^2U_0^2(1 - \omega_R/\omega_0)}{\kappa^2 + 4N^2U_0^2(1 - \omega_R/\omega_0)^2}}. \quad (20)$$

The first-order correction in $1/\kappa$ gives the dominant term of the corresponding damping rate

$$\gamma_1 = \omega_0^2 \kappa \frac{4N^2U_0^2(1 - \omega_R/\omega_0)}{[\kappa^2 + 4N^2U_0^2(1 - \omega_R/\omega_0)^2]}. \quad (21)$$

We can now compare the behavior of the two lowest eigenvalues as a function of the system parameters. As an example, let us consider the case of a relatively strong pump, $\eta^2 \gg N^2U_0\omega_R$. In this limit, the second excitation frequency ν_2 is only weakly shifted from the harmonic-oscillator frequency $2\omega_0$. On the other hand, the frequency shift of the lowest excitation ν_1 mainly depends on the ratio NU_0/κ . Since this ratio has to be larger than one in order to yield a significant frequency shift of the cavity by the atoms, Eq. (20) implies that ν_1 is strongly shifted towards zero. Simultaneously we find for the damping rates that γ_2 becomes independent of η in this limit, in contrast to γ_1 , which is proportional to ω_0 and thus proportional to η^2 . Therefore the damping rate of the first antisymmetric excitation can be increased arbitrarily by increasing the intensity of the pump field. The damping rate of the first symmetric excitation is much harder to manipulate because it is mainly governed by the optical potential per photon and thus by the quality of the cavity. On the other hand, we note that γ_2 scales proportional to N^2 , whereas γ_1 is inversely proportional to N^2 . The number of atoms thus provides another handle to change the relative size of the damping rates γ_1 and γ_2 .

Another point is worth a comment here. We emphasized in the previous section that the damping mechanism for the collective excitations in a standing-wave cavity is crucially related to the width of the matter wave function and vanishes in the semiclassical limit where the atoms are treated as point particles. In contrast to this we find that in the traveling-wave cavity the damping mechanism still exists in the semiclassical limit. In fact, our results for the oscillation frequency (20) and the damping rate (21) agree with the semiclassical results [29] if one takes formally the limit $\omega_R/\omega_0 \rightarrow 0$.

In Fig. 3 we show the excitation frequencies $\nu_{1,2}$ and the damping rates $\gamma_{1,2}$ as a function of the pump strength η^2 for both the numerical solution and the analytic approximations. We see that for the chosen parameters the approximations fit quite well apart from the values of γ_2 . This comes from the fact that we obtained the complex eigenvalues ω_n from an expansion of Eqs. (8) and (19) for small values of $|\omega_n|/\kappa \ll 1$. As we see from Fig. 3(a) this is well fulfilled for ω_1 for the chosen parameters, but $|\omega_2|/\kappa$ is of the order of one. However, in the limit of a strong pump the lowest-order term for the frequency ν_2 already gives the correct value, namely, twice the harmonic-oscillator frequency. Thus, only the imaginary part (the damping rate γ_2) of the analytic approximation deviates from the exact solution in Fig. 3. In parameter regions, where $|\omega_2|/\kappa \ll 1$, we find a much better agreement of the two solutions.

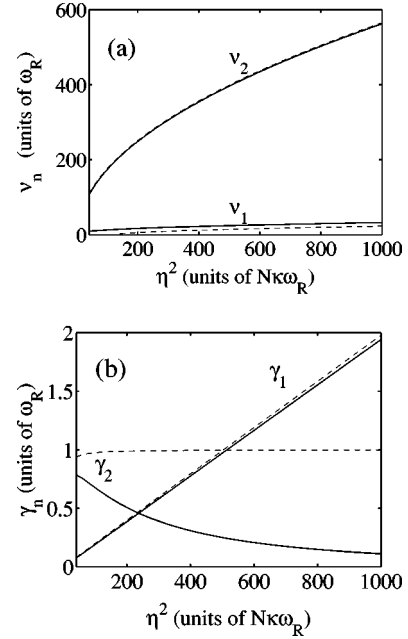


FIG. 3. Collective condensate excitations in a ring cavity: (a) frequencies ν_n and (b) decay rates γ_n vs pump strength η^2 . The parameters are $g_{coll} = \Delta_c = 0$, $NU_0 = 5\kappa$, and $\kappa = 400\omega_R$. The solid curves are obtained numerically, the dashed curves are the analytical solutions obtained in the harmonic-oscillator approximation.

IV. INTERACTING BOSE GAS

In the discussion so far we have omitted the effects of atomic interactions, as described by the collision rate g_{coll} in the GPE, on the energies and damping rates of the collective excitations. Neglecting this has allowed us to obtain analytical expressions and therefore to discuss the parameter dependence of our results explicitly. However, atomic collisions are known to play a crucial role in experimental realizations of Bose-Einstein condensates. We will now discuss the changes of the collective excitations according to collisions in a numerical example of a condensate in a ring cavity.

We show in Fig. 4 the excitation frequencies ν_n and the corresponding damping rates γ_n as a function of the collision rate g_{coll} with all other parameters fixed. The main effect on the stationary ground-state wave function [23] of a repulsive interaction between the condensed atoms is to increase the width of the wave function. Since this larger width also changes the coupling to the cavity field, we find that the steady-state photon number decreases with increasing collision rate. Consequently, the optical potential becomes more shallow and the excitation frequencies decrease. However, as we can see from Fig. 4, this argument does not hold for the lowest (antisymmetric) excitation. Here the atomic collisions counteract the strong frequency shift that we found in the previous section and ν_1 slightly increases with g_{coll} . Above a certain threshold value for g_{coll} , the atom-atom repulsion gets stronger than the confining effect of the optical potential. In this case the ground-state wave function is no longer localized and the spectrum of excitations changes into that of unbound particles where each excitation frequency is doubly degenerate.

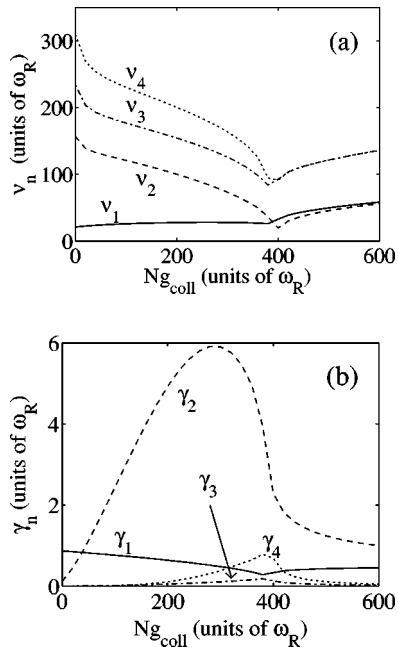


FIG. 4. (a) Frequencies ν_n and (b) decay rates γ_n of the collective excitations vs atomic collision rate g_{coll} . The parameters are $\Delta_c=0$, $NU_0=2\kappa$, $\kappa=400\omega_R$, and $\eta^2=200N\kappa\omega_R$.

Figure 4(b) shows that collisional effects have an even more important influence on the damping rates of the collective excitations. We see that the effect differs for the damping rates γ_1 and γ_2 . While γ_1 weakly decreases with increasing g_{coll} , γ_2 increases significantly over a broad range of values of g_{coll} . This is related to the fact that the damping of the symmetric excitation γ_2 depends crucially on the width of the ground-state wave function whereas the damping mechanism of the antisymmetric excitation does not, as already emphasized before. Since the major effect of atom collisions is to broaden the wave function, the resulting changes of the damping rates occur predominantly for the symmetric excitations. Note also that the atomic collisions and the stronger anharmonicity of the potential according to the lower field intensity enhance the damping of higher collective excitations, as can be seen from the damping rates γ_3 and γ_4 in Fig. 4(b).

V. CONCLUSIONS

In summary we have studied in detail the interaction of a Bose-Einstein condensate with one or two single modes in a high-finesse optical cavity in a 1D model. This relies on a small transverse extension of the condensate compared to the waist of the cavity mode. In an actual experiment this could be realized, for instance, by additional transverse trapping by

magnetic or optical means, or by a freely falling condensate, in which case our model only holds for a time scale of the order of the expansion time scale of the condensate. We have solved the coupled set of nonlinear equations of motion for the joint dynamics of the condensate and the light field numerically and compared it analytically with a simplified model based on the Lamb-Dicke expansion. We find that, even without atom-atom interaction, the oscillation frequencies are shifted with respect to their values in a fixed external potential.

For a finite cavity response time the collective excitations are damped or amplified depending on the cavity detuning, which can be easily controlled externally. We identify two distinct mechanisms depending on the spatial symmetry of the excitations. The damping mechanism in standing-wave cavities and for spatially symmetric excitations in ring cavities is due to a Sisyphus type effect, which leads to larger cavity fields at times when the condensate runs up potential hills than at times when the condensate runs down. On average this effect extracts kinetic energy from the condensate which is carried away by the cavity field. On the other hand, the damping mechanism for the spatially antisymmetric excitations is only present in a ring cavity due to the scattering of cavity photons between the two counterpropagating waves. This creates an intensity imbalance, which is counteracted by the cavity damping and hence leads to momentum dissipation.

The two damping mechanisms exhibit very distinct parameter dependences. Our analytical approximations show that in the limit of strong cavity pumping the damping rate of the spatially symmetric excitations becomes independent of the pump but scales proportional to the square of the atom number N^2 , while the damping rate of the antisymmetric excitations is proportional to the pump field intensity and inversely proportional to N^2 , which implies less stringent requirements to cavity technology.

The difference between the damping-amplification rates of excitations with different spatial symmetry could be used to manipulate a Bose-Einstein condensate in a controlled fashion. In addition, in a ring cavity setup, we can also excite oscillations by external phase and amplitude shifts of the pump light. All the effects could of course be enhanced by tailored feedback of the measured transmitted intensity onto the pump. This might give rise to useful applications of such a system in the context of quantum information and quantum computation in analogy to other recently proposed systems making use of particles in optical lattices [30–32].

ACKNOWLEDGMENTS

We thank J. I. Cirac and P. Zoller for stimulating discussions. This work was supported by the Austrian Science Foundation FWF (Project No. P13435).

[1] M. H. Anderson, J. R. Ensher, M. R. Matthews, C. E. Wieman, and E. A. Cornell, *Science* **269**, 198 (1995); C. C. Bradley, C. A. Sackett, J. J. Tollett, and R. G. Hulet, *Phys. Rev. Lett.* **75**, 1687 (1995); K. B. Davis, M.-O. Mewes, M. R. Andrews, N. J.

van Druten, D. S. Durfee, D. M. Kurn, and W. Ketterle, *ibid.* **75**, 3969 (1995).

[2] W. Ketterle, D. S. Durfee, and D. M. Stamper-Kurn, in *Proceedings of the International School of Physics Enrico Fermi*,

- edited by M. Inguscio, S. Stringari, and C. E. Wieman (IOS Press, Amsterdam, 1999).
- [3] A. S. Parkins and D. F. Walls, *Phys. Rep.* **303**, 2 (1998).
- [4] F. Dalfovo, S. Giorgini, L. P. Pitaevskii, and S. Stringari, *Rev. Mod. Phys.* **71**, 463 (1999).
- [5] E. W. Hagley, L. Deng, M. Kozuma, J. Wen, K. Helmerson, S. L. Rolston, and W. D. Phillips, *Science* **283**, 1706 (1999); M. Kozuma, L. Deng, E. W. Hagley, J. Wen, R. Lutwak, K. Helmerson, S. L. Rolston, and W. D. Phillips, *Phys. Rev. Lett.* **82**, 871 (1999).
- [6] B. P. Anderson and M. A. Kasevich, *Science* **282**, 1686 (1998).
- [7] D.-I. Choi and Q. Niu, *Phys. Rev. Lett.* **82**, 2022 (1999).
- [8] D. Jaksch, C. Bruder, J. I. Cirac, C. W. Gardiner, and P. Zoller, *Phys. Rev. Lett.* **81**, 3108 (1998).
- [9] K. Berg-Sørensen and K. Mølmer, *Phys. Rev. A* **58**, 1480 (1998).
- [10] K.-P. Marzlin and W. Zhang, *Phys. Rev. A* **59**, 2982 (1999).
- [11] L. V. Hau, S. E. Harris, Z. Dutton, and C. H. Behroozi, *Nature (London)* **397**, 594 (1999).
- [12] S. Inouye, A. P. Chikkatur, D. M. Stamper-Kurn, J. Stenger, D. E. Pritchard, and W. Ketterle, *Science* **285**, 571 (1999); *Appl. Phys. B: Lasers Opt.* **69**, 347 (1999).
- [13] M. R. Matthews, B. P. Anderson, P. C. Haljan, D. S. Hall, C. E. Wieman, and E. A. Cornell, *Phys. Rev. Lett.* **83**, 2498 (1999).
- [14] K. W. Madison, F. Chevy, W. Wohlleben, and J. Dalibard, *Phys. Rev. Lett.* **84**, 806 (2000).
- [15] G. Nogues, A. Rauschenbeutel, S. Osnaghi, M. Brune, J. M. Raimond, and S. Haroche, *Nature (London)* **400**, 239 (1999); A. Rauschenbeutel *et al.*, *Phys. Rev. Lett.* **83**, 5166 (1999).
- [16] P. Münstermann, T. Fischer, P. Maunz, P. W. H. Pinkse, and G. Rempe, *Phys. Rev. Lett.* **82**, 3791 (1999); G. Rempe *et al.* in *Laser Spectroscopy 14th International Conference ICOLS99*, edited by R. Blatt, J. Eschner, D. Leibfried, and F. Schmidt-Kaler (World Scientific, Singapore, 1999).
- [17] J. Ye, D. W. Vernooy, and H. J. Kimble, *Phys. Rev. Lett.* **83**, 4987 (1999); C. J. Hood, M. S. Chapman, T. W. Lynn, and H. J. Kimble, *ibid.* **80**, 4157 (1998).
- [18] J. F. Corney and G. J. Milburn, *Phys. Rev. A* **58**, 2399 (1998).
- [19] C. K. Law and N. P. Bigelow, *Phys. Rev. A* **58**, 4791 (1998).
- [20] E. V. Goldstein, E. M. Wright, and P. Meystre, *Phys. Rev. A* **57**, 1223 (1998); E. S. Lee *et al.*, *ibid.* **60**, 4006 (1999).
- [21] P. Horak, G. Hechenblaikner, K. M. Gheri, H. Stecher, and H. Ritsch, *Phys. Rev. Lett.* **79**, 4974 (1997); G. Hechenblaikner, M. Gangl, P. Horak, and H. Ritsch, *Phys. Rev. A* **58**, 3030 (1998).
- [22] M. Gangl and H. Ritsch, *Phys. Rev. A* **61**, 011402 (2000); *Eur. Phys. J. D* **8**, 29 (2000); *Phys. Rev. A* **61**, 043405 (2000).
- [23] P. Horak, S. M. Barnett, and H. Ritsch, *Phys. Rev. A* **61**, 033609 (2000).
- [24] S. Stringari, *Phys. Rev. Lett.* **77**, 2360 (1996).
- [25] V. M. Perez-Garcia, H. Michinel, J. I. Cirac, M. Lewenstein, and P. Zoller, *Phys. Rev. Lett.* **77**, 5320 (1996).
- [26] L. You, W. Hoston, and M. Lewenstein, *Phys. Rev. A* **55**, R1581 (1997).
- [27] Y. Castin and R. Dum, *Phys. Rev. A* **57**, 3008 (1998).
- [28] M. G. Moore and P. Meystre, *Phys. Rev. A* **59**, R1754 (1999); M. G. Moore, O. Zobay, and P. Meystre, *ibid.* **60**, 1491 (1999).
- [29] M. Gangl, P. Horak, and H. Ritsch, *J. Mod. Opt.* **47**, 2741 (2000).
- [30] D. Jaksch, H.-J. Briegel, J. I. Cirac, C. W. Gardiner, and P. Zoller, *Phys. Rev. Lett.* **82**, 1975 (1999).
- [31] G. K. Brennen, C. M. Caves, P. S. Jessen, and I. H. Deutsch, *Phys. Rev. Lett.* **82**, 1060 (1999).
- [32] A. Hemmerich, *Phys. Rev. A* **60**, 943 (1999).